Joint Rate-Brightness Control using Variable Rate MPPM for LED Based Visible Light Communication Systems

Abu Bakar Siddique and Muhammad Tahir, *Member, IEEE*

***Abstract*—LED based lighting systems provide an opportunity for data transmission in addition to their traditional use as source of illumination. Brightness control is required to achieve either desired level of illumination or to achieve energy conservation. Conventionally, simultaneous data transmission as well as brightness control is achieved using two different modulation schemes. Either pulse width modulation or pulse amplitude modulation is used for brightness control and some variants of pulse position modulation are employed for data transmission. The need for two different modulation schemes, to meet the dual objective, makes the system design complex. In this paper we propose variable-rate multi-pulse-position-modulation (VR-MPPM), for LED based visible light communication system, to achieve joint brightness control and data transmission. The proposed approach eradicates the need for either pulse width modulation or pulse amplitude modulation and still achieves the brightness control. Encoder and decoder algorithms for VR-MPPM realization are developed and are implemented on the hardware testbed. Experimental results revealing the effect of brightness level variation on symbol error rate are also provided. Existence of an underlying trade-off between achievable resolution for brightness control and the corresponding successful data transmission rate is recognized. To exploit this trade-off, an optimization problem is formulated.**

***Index Terms*—Visible light communication, multi pulse position modulation, variable rate MPPM, brightness control.**

I. Introduction

THE lighting industry is rapidly transitioning toward light emitting diode (LED) based devices and is expected to overtake conventional illumination technologies (e.g. incandescent, gas-discharge etc.) in near future [1]. LEDs offer many advantages including high efficacy, longer life, low maintenance [2] as well as faster operation. Using white LEDs for lighting not only allows control for brightness but also provide an opportunity for high speed data transmission. Despite the fact that the switching frequency of white LEDs is slower than that of colored counterpart, yet they can support data rates on the order of Mbps. This makes them potential candidate for many high speed, short range, line-of-sight, data transmission applications.

Manuscript received November 29, 2012; revised March 31 and June 6, 2013; accepted June 21, 2013. The associate editor coordinating the review of this paper and approving it for publication was Y. Zeng.

A. B. Siddique is with the University of Management and Technology Lahore, Pakistan (e-mail: mabs239@gmail.com).

M. Tahir is with the Department of Electrical Engineering, University of Engineering and Technology Lahore, and the Al-Khawarizmi Institute of Computer Science, Pakistan (e-mail: mtahir@uet.edu.pk).

Part of this paper appeared in the IEEE Consumer Communications and Networking Conference, 2011.

Digital Object Identifier 10.1109/TWC.2013.072613.121888

Two objectives of data transmission and brightness control are mostly handled separately in the literature. To achieve the objective of brightness control, one of the widely adopted solution is based on pulse-width-modulation (PWM) [3], [4], which can provide any desired brightness level ranging from 0% to 100%. Some other applications employ pulse amplitude modulation (PAM) [5] for brightness control. A continuous variation of pulse duty cycle in case of PWM and pulse amplitude in case of PAM render them unsuitable for digital data transmission. On the other hand, the modulation techniques proposed for data transmission aim to either improve power efficiency (e.g. pulse position modulation (PPM)) or enhance the bandwidth efficiency (e.g. multi-pulse-position-modulation (MPPM)) [6], [7], [8]. The solution proposed in [9] tries to achieve both power as well as bandwidth efficiency using a transmission scheme based on rate-adaptive MPPM. From the above cited literature one can conclude that the key focus of the research in this area is on either improving the power or the bandwidth efficiency, but little attention is dedicated to brightness control. This is also true due to the fact that the modulation schemes for data transmission were originally designed for free space optical communications based on infra-red (IR) transmissions and did not require any brightness control mechanism.

To achieve simultaneous data transmission and brightness control, only few approaches have been proposed in the literature. Among those, variable PPM (VPPM) [10], variable on-off keying (VOOK) [11] and overlapping PPM (OPPM) [12], are of importance. These modulation schemes will be discussed in Section IV and will also be used for performance comparison. Some other related works vying for joint brightness control and data transmission, include [13], [14]. In [13], PWM is used for brightness control, while data transmission is achieved by making the frequency of the PWM relatively large compared to the symbol duration. A second approach is also proposed in [13] using pulse position modulation for data transmission and an appropriate DC level is added to the PPM pulses to achieve the desired brightness. This approach is highly bandwidth inefficient, due to the usage of high frequency switching pulses, while the actual data transmission rate is quite low. In another related work [14], the authors have proposed a tunable hybrid modulation scheme based on pulse-amplitude and pulse position modulation to guarantee system performance by maintaining power and bandwidth efficiency. This hybrid modulation scheme has the

TABLE I
EXAMPLE VARIABLE-RATE MPPM FOR $n = 8$

Parameter r	brightness-index $\frac{r}{n}$	no. of codes ${}^nC_r$	bits/symbol $\lfloor \log_2({}^nC_r) \rfloor$
1	0.125	8	3
2	0.250	28	4
3	0.375	56	5
4	0.500	70	6
5	0.625	56	5
6	0.750	28	4
7	0.875	8	3

potential of being used for simultaneous brightness control and data transmission, however, at low brightness levels the data transmission capability of the proposed method in [14] is hampered due to the reduction in pulse amplitudes, which will result in large bit errors. The amplitude variations for brightness control (e.g. in case of PAM) for small values of B_I will result in lower magnitude pulses leading to poor signal to noise ratio (SNR).

In this paper, we propose variable-rate MPPM (VR-MPPM) to achieve brightness control as well as data transmission simultaneously and have compared its performance with existing approaches. It provides a flexible yet efficient solution to attain joint brightness control and data transmission. The proposed approach neither requires any high frequency subcarrier for data transmission nor it needs PWM signaling for brightness control. In contrast to PAM, the pulse amplitude remains unchanged in case of VR-MPPM, independent of brightness index and SNR does not degrade [15]. One limitation of the proposed scheme is that actual data transmission rate is not same at all the brightness levels. The proposed VR-MPPM based VLC system can be used for indoor applications throughout the day. The solution is equally useful for outdoor applications, particularly at night. One such application is the use of street lights to broadcast local map information along with current road congestion situation to guide the people. Rest of the paper is organized as follows.

In Section II we outline the proposed variable-rate multi-pulse-position-modulation scheme. Iterative algorithms are developed for sequential encoding and decoding of information symbols. For the proposed VR-MPPM, performance bounds in terms of code-rate are also derived. In Section III, we formulate an optimization problem, to exploit the underlying trade-off between brightness resolution and successful data transmission rate using VR-MPPM. Section IV outlines details of experimental implementation and performance evaluation. Results are provided to show the effectiveness of the proposed VR-MPPM in achieving joint brightness control and data transmission. Finally we conclude our findings in Section V.

II. VARIABLE-RATE MPPM

The proposed joint brightness control and data transmission solution can be explained in the context of multi-pulse-position-modulation. The information carrying capability of MPPM is affected by two factors; 1) total number of slots per information symbol and 2) the number of pulsed slots per symbol. PPM as a special case of MPPM uses just one pulsed slot and carries minimum information per symbol duration. For an n slot symbol frame, if r of those slots mark the presence of a pulse and $n - r$ slots mark the pulse absence, then the total number of distinct combinations, which can be used for symbol encoding, are computed as ${}^nC_r = \frac{n!}{r!(n-r)!}$ for $r \in \{1, 2, \cdots, n-1\}$. The number of bits required to encode ${}^nC_r$ symbols is given by $\log_2({}^nC_r)$ that can provide a *code-rate* of $\frac{1}{n}\log_2({}^nC_r)$. Of the $\log_2({}^nC_r)$ bits, $\lfloor \log_2({}^nC_r) \rfloor$ bits are useful for binary data encoding. For a fixed value of parameter n, the number of symbols that can be encoded depends on the current choice of parameter r, which in turn is adjusted for desired brightness level. Since the achievable code-rate is not same at different brightness levels, we name the proposed scheme as variable-rate MPPM.

Choosing the parameter $r \in \{1, 2, \cdots, n-1\}$ sets the limits for achievable brightness level with $r = 1$ corresponds to minimum brightness while $r = n - 1$ provides the maximum brightness level. We define *brightness-index*, B_I, as the ratio $\frac{r}{n}$, which for a given pair (n, r) is the measure of DC average of the signal. The two other possible values of parameter r i.e. $r = 0$ (corresponding to light OFF) and $r = n$ (corresponding to light ON with maximum brightness) are not useful, since data transmission is not achievable for these two cases. Different parameters related to variable-rate MPPM encoding are tabulated in Table I for $n = 8$. Next we outline the key features of the proposed variable-rate MPPM:

- The resolution of brightness control increases by increasing the value of parameter n.
- For a given value of parameter n, bandwidth efficiency is minimum at $r = 1$ (corresponding to the minimum brightness level) as well as $r = n - 1$ (corresponding to the maximum brightness level) and is termed as worst case bandwidth efficiency.
- The worst case bandwidth efficiency degrades further as the value of parameter n is increased. This also points toward the trade-off between brightness control resolution (which increases as n increases) and worst case bandwidth efficiency (which reduces as n is increased).
- Whenever new value for parameter r is selected by the transmitter to obtain desired brightness level, decoding can be performed without conveying this information to the decoder. However, in this mode of operation the decoder is vulnerable to perceive symbol errors as a change in the brightness level occurs.
- The maximum value of the parameter n that can be used is based on the flickering effect. At higher data rates, with a nominal value of n, this effect will not be pronounced. Since the switching frequencies used for data transmission are on the order of MHz, flicker can only be an issue if the transmitted signal is not DC balanced for long time intervals. Flickering frequencies above 50 Hz are not perceived by human eye. For the proposed VR-MPPM, inter-frame DC imbalance does not exist when the frames use same brightness index. On the other hand intra-frame DC imbalance can become an issue only if the selected frame size is too large (approximately larger than 2×10^4 bits for 1 Mbps transmission rate). However,

TABLE II
SYMBOL ENCODING AND DECODING MATRIX

$r \diagdown i$	pv_{n-1}	pv_{n-2}	$\cdots$	pv_{n-i}	$\cdots$	pv_2	pv_1	pv_0
$n-1$	${}^{n-1}C_{n-1}$	0	$\cdots$	0	$\cdots$	0	0	0
$n-2$	${}^{n-1}C_{n-2}$	${}^{n-2}C_{n-2}$	$\cdots$	0	$\cdots$	0	0	0
$\vdots$	$\vdots$	$\vdots$	$\cdots$	$\vdots$	$\cdots$	$\vdots$	$\vdots$	$\vdots$
r	${}^{n-1}C_r$	${}^{n-2}C_r$	$\cdots$	${}^{n-i}C_r$	$\cdots$	0	0	0
$\vdots$	$\vdots$	$\vdots$	$\cdots$	$\vdots$	$\cdots$	$\vdots$	$\vdots$	$\vdots$
2	${}^{n-1}C_2$	${}^{n-2}C_2$	$\cdots$	${}^{n-i}C_2$	$\cdots$	${}^{2}C_2$	0	0
1	${}^{n-1}C_1$	${}^{n-2}C_1$	$\cdots$	${}^{n-i}C_1$	$\cdots$	${}^{2}C_1$	${}^{1}C_1$	0

the practical frame size used, will be on the order of 10^2, as discussed in Section IV, and the flickering issue is almost non-existent for practical situations.

The proposed VR-MPPM allows a symbol to be encoded for any value of r from 1 to $n-1$ and the choice of parameter r is based on the desired brightness level. The information symbol s_k, with $k \in \{0, 1, 2, \cdots, 2^{\lfloor \log_2({}^nC_r) \rfloor} - 1\}$, is encoded using a codeword of size n. The key aspect to understand the proposed scheme is the calculation of the *place-value* corresponding to the pulsed-slot location in the codeword. The place-value of the pulsed-slot in the encoded signal depends not only on its position in the codeword but also on the current value of parameter r, controlling the total number of pulsed slots. Due to this fact, it is different from ordinary binary coding, where the place-value of a pulsed-slot depends on its absolute position in the codeword. A symbol s_k can be coded by using an n slot codeword with r number of pulsed-slots and the resulting encoded symbol is represented by (n, r, s_k). To illustrate encoding/decoding procedure we first construct Table II, where each row corresponds to a particular value of parameter r. For r^{th} row and i^{th} column with $r \in \{1, 2, \cdots, n-1\}$ and $i \in \{1, 2, \cdots, n\}$ the corresponding entry (r, i) in the Table II is obtained as

$$(r,i) = \begin{cases} {}^{n-i}C_r & r \le (n-i) \\ 0 & r > (n-i) \end{cases} . \tag{1}$$

A. Encoder/Decoder Example

We provide a simple illustration for $n = 5$ to explain the encoding and decoding procedure. For that purpose, Table II is evaluated for $n = 5$ and the result is given in Table III. Let the desired brightness-index is 0.6 and the symbol to be encoded is $s_k = 2$, then we need to use the codeword corresponding to $(n, r, s_k) = (5, 3, 2)$. To start encoding, we begin at the intersection of column corresponding to pv_4 and row corresponding to $r = 3$, which has a place-value of 4 as seen from Table III. Since the place-value of 4 is larger than $s_k = 2$ we move to the intersection of column pv_3 and row corresponding to $r = 3$ with a place-value of 1. Since the place-value is less than s_k, we decrement this value from s_k to have $s_k = 1$ and move to the intersection of column pv_2 and row $r = 2$ with a place-value of 1. Again we subtract the place-value of 1 from s_k to have a new value of $s_k = 0$ and move to the intersection of column pv_1 and row $r = 1$ with a place-value of 1. This place-value should not be subtracted from s_k as s_k can not be negative, which is achieved by moving to the column pv_0 but staying at the row $r = 1$. Finally, since the number of 1's in the partially constructed codeword is two we need to have an additional 1 to achieve the desired $B_I = 0.6$. This is achieved by assigning 1 to the slot corresponding to the column pv_0 and row $r = 1$. This gives us the codeword $(5, 3, 2) = [0\ 1\ 1\ 0\ 1]$ for transmitting symbol $s_k = 2$ with brightness-index of 0.6 and using a codeword with $n = 5$ slots. The encoder implementation follows MSB first transmission. It should be noted that for this example the possible brightness indices are 0.2, 0.4, 0.6 and 0.8. A set of codewords for different values of parameter B_I and $n = 5$, which can be used for binary encoding, are tabulated in Table IV. To achieve higher brightness-control resolution we need to increase the value of parameter n. A pseudo-code implementing the data encoding procedure described above is outlined in the Algorithm 1. For a given brightness index, the proposed encoding algorithm performs a unique mapping from decimal to a set of n binary digits of which r digits are ones [16].

TABLE III
SYMBOL ENCODING ILLUSTRATION

$r \diagdown i$	pv_4	pv_3	pv_2	pv_1	pv_0
4	1	0	0	0	0
3	$4^{(s_k=2)}$	$1^{(s_k=2)}$	0	0	0
2	6	3	$1^{(s_k=1)}$	0	0
1	4	3	2	$1^{(s_k=0)}$	$0^{(s_k=0)}$
$(5, 3, 2)$	0	1	1	0	1

Two different implementations of the decoder are possible. For proper decoder operation, it is assumed that symbol synchronization is achieved as discussed in [17]. The first decoder algorithm, D1, follows LSB first decoding and it is required that one complete codeword is received before the decoding can start. However, decoder does not require the prior knowledge of brightness index rather it is calculated locally at the decoder by counting the number of pulsed slots. To construct the symbol value, we start with the least significant bit. Now for i^{th} bit location in the codeword with a value of 1 the variable r is incremented by one and current symbol value s_k is incremented by pv_{i-1}, corresponding to updated value of r. The value of pv_{i-1} can be fetched from

Algorithm 1: Implementation for Encoder

Input: Variables $n,\ r,\ s_k$
Output: Encoded codeword cw
while $n > 0$ **do**
  if $0 < r < n$ **then**
    $y = {}^{n-1}C_r$
  else
    $y = 0$
  if $y \leq s_k$ **then**
    $s_k = s_k - y$
    $cw[n] = 1$
    $r = r - 1$
  else
    $cw[n] = 0$
  $n = n - 1$

TABLE IV
ENCODING SEQUENCES FOR $n = 5$

s_k	$B_I = .8$	$B_I = 0.6$	$B_I = 0.4$	$B_I = 0.2$
0	01111	00111	00011	00001
1	10111	01011	00101	00010
2	11011	01101	00110	00100
3	11101	01110	01001	01000
4	-	10011	01010	-
5	-	10101	01100	-
6	-	10110	10001	-
7	-	11001	10010	-

an already stored lookup table or can be calculated at runtime. Following this procedure for each bit location with a value of '1', the symbol value for the codeword is obtained as

$$\begin{aligned} s_k &= 0 + (pv_3|_{r=3})(1) + (pv_2|_{r=2})(1) \\ &\quad + 0 + (pv_0|_{r=1})(1) \end{aligned}$$

The second implementation of decoder, D2, just like encoder, follows MSB first decoding, but it requires prior knowledge of parameter B_I. In case of LSB first decoding, the decoder always starts corresponding to pv_0 column and $r = 1$ row (see Table II) and as a result does not require the knowledge of B_I. However, in case of MSB first decoding, the decoder starts at pv_{n-1} column but does require the knowledge of B_I to determine r to select the starting row. In this case, decoding can start immediately after the reception of first bit i.e. MSB unlike LSB first decoding which requires complete reception of one codeword before decoding can start. The pseudo codes for D1 and D2 are provided in Algorithm 2.

In case of bit errors, D1 decoding algorithm might lead to the scenario where the number of decoded bits are either larger or smaller than the actual bits transmitted. This can lead to the wrong marking of symbol boundaries in the decoded sequence and will require the higher layer (e.g. link layer) to handle this scenario. Since the need for brightness level change arises occasionally, a possible solution to this problem can be obtained by keeping track of the brightness index estimated from the number of ones per symbol in the received codeword. However the above mentioned problem does not arise when we use D2 decoding algorithm. The D2 algorithm is capable of detecting all types of bit errors except those cases of even numbered bit errors where half of the errors occur due to

Algorithm 2: Decoding Algorithms

Decoder Algorithm D1 (does not require B_I)

Input: Codeword cw of length n
Output: Data symbol s_k, r
for $i \leftarrow 1$ **to** n **do**
  if $cw[i] == 1$ **then**
    if $i > r$ **then**
      $s_k = s_k + {}^{i-1}C_r$
    $r = r + 1$

Decoder Algorithm D2 (requires B_I)

Input: Codeword cw of length n and r
Output: Data symbol s_k
for $i \leftarrow n$ **to** 1 **do**
  if $cw[i] == 1$ **then**
    if $i > r$ **then**
      $s_k = s_k + {}^{i-1}C_r$
    $r = r - 1$

ones decoded wrongly as zeros and the other half are due to zeros decoded as ones. Additionally, for D2 algorithm, symbol boundaries in case of bit errors are not affected, because the number of decoded bits are always equal to the number of transmitted bits.

The complexity of both the encoder and decoder implementations, taking into account the calculation of ${}^nC_r$ is $O(n^2)$. The time complexity can be reduced to $O(n)$ by precalculating and storing ${}^nC_r$ in a matrix. The memory size required for storing this array will be proportional to $O(n^2)$.

B. Performance Bounds

Since brightness control is one of the key objectives, we observe how tuning to different brightness levels and the choice of n, affects the achievable code rate. It should be noted that increasing n improves brightness resolution and the maximum code-rate is achieved for $r \to \frac{n}{2}$. Now code-rate upper bound, R_{max}, for $n \to \infty$ is obtained as

$$R_{max} = \lim_{\substack{r \to \frac{n}{2} \\ n \to \infty}} \frac{1}{n} \log_2 \left(\begin{array}{c} n \\ r \end{array} \right). \tag{2}$$

Defining $n = 2n'$ and letting $r = n'$, (2) becomes

$$\begin{aligned} R_{max} &\approx \lim_{n' \to \infty} \frac{1}{2n'} \log_2 \left(\frac{2^{2n'}}{\sqrt{\pi n'}} \right) \\ &= \lim_{n' \to \infty} 1 - \frac{\log_2(\pi n')}{4n'} \\ &= 1. \end{aligned} \tag{3}$$

In (3), first expression follows from Stirling's approximation, $\binom{2n'}{n'} \approx \frac{2^{2n'}}{\sqrt{\pi n'}}$ and the final expression is obtained by using L'Hopital's rule. Similarly the code-rate lower bound, R_{min} is obtained as

$$\begin{aligned} R_{min} &= \lim_{\substack{r \to n-1 \\ n \to \infty}} \frac{1}{n} \log_2 \left(\begin{array}{c} n \\ r \end{array} \right) \\ &= \lim_{n \to \infty} \frac{1}{n} \log_2(n) \\ &= 0. \end{aligned} \tag{4}$$

From practical viewpoint, the bounds might not be achievable when using binary encoding i.e the number of symbols to be encoded are always equal to 2^l. For that case the lower and upper bounds are evaluated by modifying the expression for code-rate as $\frac{1}{n}\lfloor \log_2({}^nC_r) \rfloor$.

C. Power and Spectral Efficiency Analysis

To compare the power and spectral efficiency of VR-MPPM we have selected VPPM, VOOK and OPPM, because these modulations can achieve data transmission as well as brightness control simultaneously. VPPM can be viewed as a combination of pulse width modulation (PWM) for dimming control and 2-PPM for data transmission. In VOOK, brightness is controlled by varying data duty cycle, $\delta = \frac{\tau}{T}$. Each symbol duration is divided into T slots and τ slots are filled with either zero or one depending on the value of data bit being transmitted. The $T-\tau$ slots are filled with the filler bits with either ones or zeros, which is controlled by the required brightness index [11]. Both VPPM and VOOK can transmit one bit of information in each symbol duration. OPPM is defined as a special case of MPPM, where the r ones are consecutive i.e. each symbol consisting of n time slots contains only one rectangular pulse spanning r slots and each pulse starts at any of the first $L = n - r + 1$ slots [12]. The number of bits that can be transmitted using OPPM is $\log_2(L)$.

The normalized spectral efficiency of VR-MPPM is defined as the ratio $\frac{R_b}{B_{MPPM}}$, where R_b is the bit rate (in bits per sec) and B_{MPPM} is the bandwidth defined approximately as the inverse of one pulse duration. Based on this definition we obtain the normalized spectral efficiency for VR-MPPM as $\frac{R_b}{B_{MPPM}} = \frac{\lfloor \log_2 \binom{n}{r} \rfloor}{n}$ [18]. To simplify power efficiency analysis high-SNR assumption is made, which implies that probability of error is dominated by minimum distance between any pair of codewords. Based on this assumption the power required by VR-MPPM, P_{MPPM}, to achieve same bit error rate as that of OOK is approximated as $P_{MPPM} = (d_{OOK}/d_{min})P_{OOK}$ [18], where d_{OOK} and d_{min} are minimum Hamming distances for OOK and VR-MPPM respectively. Now power requirement for MPPM to achieve given bit error rate, same as that of OOK, is given by

$$\frac{P_{MPPM}}{P_{OOK}} = r\sqrt{\frac{2}{n\log_2\binom{n}{r}}}$$

Spectral and power efficiency results for VPPM and VOOK are obtained in [11] and for that of OPPM in [12]. The power and spectral efficiency results for VR-MPPM and other modulation schemes are tabulated in Table V.

We mention that multi-level PAM can be a promising choice for modulation to meet high data rate requirements under high brightness conditions. However, from a practical viewpoint in the context of LED based lighting, multi-level PAM poses two problems when it is used for controlling the magnitude of LED drive current. The first problem is of the chromatic shift with changing drive current and the second one arises from non-linear relationship between the LED drive current and the achieved brightness level [19] [20].

III. Performance Optimization

It is mentioned above that an improvement in the brightness resolution requires an increase in the value of parameter n. Since every symbol is encoded using n slots, increasing n arbitrarily will lead to higher symbol errors at the decoder output. To observe this, assume that the decoding error probability of a slot without pulse is denoted by $\bar{p}_1$ and that of a slot with pulse is $\bar{p}_2$. In VLC system when the transmission follows line-of-sight path, error probabilities $\bar{p}_1$ and $\bar{p}_2$ can be obtained by modeling the photo-detector behavior as photon-counting process following Poisson distribution [21], [8]. Let μ_s and μ_b, respectively, denote the mean photon count, due to light source in a pulsed slot and due to background-noise and photo-detector dark-current in a slot without pulse, [21]. Probability, $\bar{p}_2$, of accumulating at most α photons in a pulsed slot, corresponding to bit '1' transmission, is given by $\bar{p}_2 = \sum_{k=0}^{\alpha} e^{(\mu_s+\mu_b)}\frac{(\mu_s+\mu_b)^k}{k!}$. On the other hand $\bar{p}_1$ is given by the probability of accumulating at least α photons in a slot without pulse, corresponding to bit '0' transmission and is given by $\bar{p}_1 = \sum_{k=\alpha}^{\infty} e^{(\mu_b)}\frac{(\mu_b)^k}{k!}$. Now the probability of correctly receiving a symbol, denoted by p_c, is given by

$$p_c = (1-\bar{p}_1)^{n-r}(1-\bar{p}_2)^r, \tag{5}$$

where r is the number of pulsed slots in an n slot frame. When n increases, p_c decreases resulting in performance degradation. This indicates the existence of an underlying trade-off between the achievable brightness-resolution and the symbol successful transmission rate. To achieve this trade-off optimally, we define an objective function which tries to maximize p_c as well as brightness-resolution and the resulting optimization problem is given by

$$\begin{aligned} \textbf{maximize} \quad & g(n) = n(1-\bar{p}_1)^{n-r}(1-\bar{p}_2)^r, \\ \textbf{subject to} \quad & 0 < r < n, \quad 0 \le \bar{p}_1, \bar{p}_2 < 1. \end{aligned} \tag{6}$$

The objective function is characterized to find out that the solution to the optimization problem in (6) is optimal globally or not. For that matter, we consider two separate scenarios. In first scenario it is required that the ratio r/n is constant resulting in the desired B_I for different frame sizes. In the second case we require the parameter r to be fixed, which results in variable B_I for different values of parameter n, providing desired level of brightness resolution. Additionally, we relax parameter n in (6) to be a real number.

A. Case for Constant B_I

Since $B_I = \frac{r}{n}$, we require $\frac{r}{n} = k_1$ and k_1 is a real positive constant. In this case the objective function in (6) becomes

$$g(n) = np_1^{n(1-k_1)}p_2^{k_1 n},$$

where $p_i = 1-\bar{p}_i$ for $i = \{1, 2\}$. To characterize the objective function, $g(n)$, we evaluate its second derivative as

$$g''(n) = p_1^{n(1-k_1)}p_2^{k_1 n}\ln(p_1^{1-k_1}p_2^{k_1})\left(n\ln(p_1^{1-k_1}p_2^{k_1}) + 2\right). \tag{7}$$

TABLE V
POWER AND SPECTRAL EFFICIENCY OF MODULATION SCHEMES

Modulation	Normalized Power	Spectral Efficiency
VPPM	$\sqrt{\frac{2}{1-B_I}}$	$B_I \quad 0 \le B_I \le 0.5$ $1-B_I \quad 0.5 \le B_I \le 1$
VOOK	$\sqrt{\frac{2}{1-B_I}}$	$2B_I \quad 0 \le B_I \le 0.5$ $2(1-B_I) \quad 0.5 \le B_I \le 1$
OPPM	$r\sqrt{\frac{2}{n\log_2(n-r+1)}}$	$B_I \log_2(n-r+1) \quad 0 \le B_I \le 0.5$ $(1-B_I)\log_2(n-r+1) \quad 0.5 \le B_I \le 1$
MPPM	$r\sqrt{\frac{2}{n\log_2\binom{n}{r}}}$	$\frac{\log_2\binom{n}{r}}{n}$

Observing the expression in (7), the objective function is characterized as

$$g(n) = \begin{cases} \text{concave i.e. } g''(n) \le 0 & \frac{2}{|\ln(p_1^{1-k_1}p_2^{k_1})|} \ge n \\ \text{convex i.e. } g''(n) \ge 0 & \frac{2}{|\ln(p_1^{1-k_1}p_2^{k_1})|} \le n \end{cases}, \tag{8}$$

From the result in (8), it can be concluded that the objective function, $g(n)$, is quasi-concave [22]. For quasi-concave functions, it is known that locally optimal solutions are not globally optimal [22]. However, the super-level sets of a quasi-concave function are convex and can be represented using a family of concave inequalities. Let $\phi(\alpha) : \mathbb{R} \to \mathbb{R},\ \alpha \in \mathbb{R}$, be a family of concave functions that satisfy

$$g(n) \ge \alpha \iff \phi(\alpha) \ge 0. \tag{9}$$

A candidate solution that satisfy (9) can be obtained from $\phi(\alpha) = \ln n + n\ln(p_1^{1-k_1}p_2^{k_1}) - \ln\alpha$. The solution to the optimization problem in (6) is now obtained by solving the concave feasibility problem in (10) using bisection method.

$$\begin{aligned} \textbf{find} \quad & n \\ \textbf{subject to} \quad & \ln n + n\ln(p_1^{1-k_1}p_2^{k_1}) - \ln\alpha \ge 0 \\ & 0 < k_1 < n, \quad 0 < p_1, p_2 \le 1. \end{aligned} \tag{10}$$

B. Case for Constant r

Define $r = k_2$, where k_2 is a real positive constant. The corresponding objective function now can be rewritten as

$$g(n) = np_1^n \left(\frac{p_2}{p_1}\right)^{k_2}.$$

Following the procedure in the previous case of constant B_I, we can verify the quasi-convexity of objective function in this case as well. The optimal value of n now can be readily obtained by replacing $p_1^{1-k_1}p_2^{k_1}$ with p_1 in (7) and (10).

IV. PERFORMANCE EVALUATION RESULTS

We first evaluate VR-MPPM, numerically, for its optimal trade-off between achievable brightness resolution in terms of n and symbol successful transmission rate in terms of $\bar{p}_1$ and $\bar{p}_2$. The optimal word length n^* as a function of pulse decoding error probability $\bar{p}_1$ and B_I, is shown in Fig. 1. From Fig. 1 we observe that the cross-over point for different values of B_I corresponds to the case $\bar{p}_1 = \bar{p}_2$. In other words, when $\bar{p}_1 = \bar{p}_2$, n^* is independent of brightness-index, B_I. It can also be observed from Fig. 1 that the optimal frame size is less than 10^3 bits for practical range of pulse decoding error probabilities. The result in Fig. 2 shows the variation in the choice of optimal word length n^* as a function of pulse decoding error probability $\bar{p}_1$ and $\bar{p}_2$ for $B_I = 0.5$.

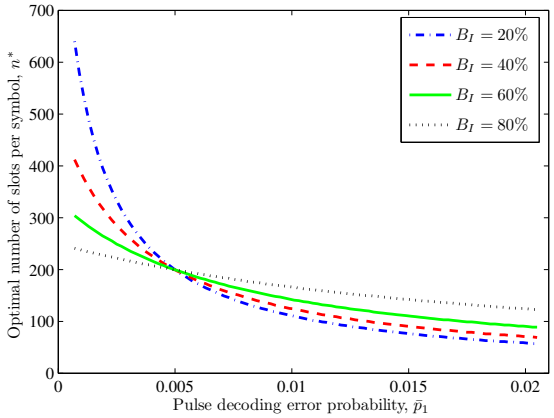

Fig. 1. Choice of optimal word length, n^*, as a function of pulse decoding error probability $\bar{p}_1$. For this result $\bar{p}_2 = 0.005$ is used.

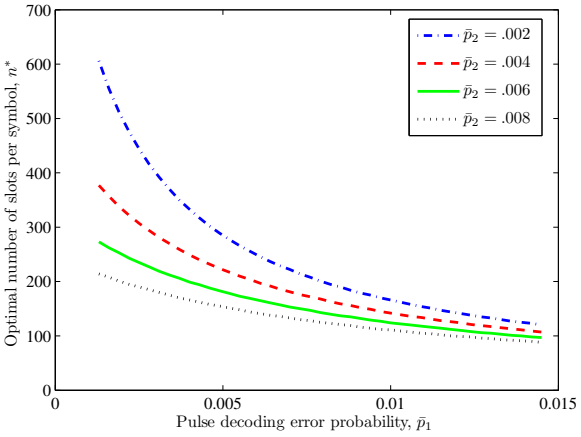

Fig. 2. Choice of optimal word length, n^*, as a function of pulse decoding error probability $\bar{p}_1$. For this result $B_I = 0.5$ is used.

A. Performance Comparison

We evaluate the power and spectral efficiency of different modulation schemes, including VR-MPPM, as a function of brightness-index. The power efficiency comparison is based on optical power. Normalized power efficiency results are shown in Fig. 3, where normalization is done by OOK power. The

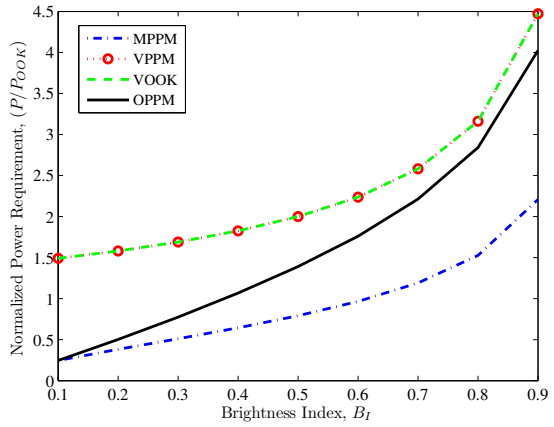

Fig. 3. Normalized power efficiency as a function of modulation index for different modulation schemes. $n = 10$ is used for these results.

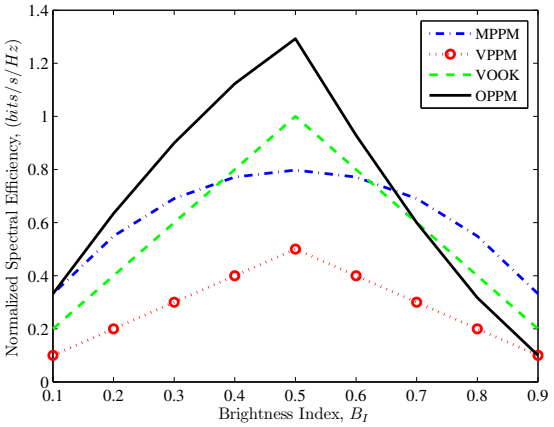

Fig. 4. Normalized spectral efficiency as a function of modulation index for different modulation schemes for $n = 10$.

superior performance of VR-MPPM compared to other modulation schemes can be observed from Fig. 3. Power efficiencies of VR-MPPM and OPPM become equal for minimum value of brightness-index, $B_I = 0.1$, because both of them reduce to PPM for this case. Spectral efficiency as a function of brightness-index, for different modulation schemes, is shown in Fig. 4. The spectral efficiency of VR-MPPM and OPPM is same for minimum value of brightness-index due to the above mentioned reason. For small values of B_I OPPM is superior, however, VR-MPPM is more spectral efficient for larger values of B_I. Overall we can observe the superiority of VR-MPPM compared to other modulation schemes when considering both power and spectral efficiency. We observe that omission of transmission intervals to achieve brightness control is wasteful from communications perspective.

B. Experimental Results

For real-time experimentation and performance evaluation, the proposed VR-MPPM encoder and decoder algorithms were implemented for variable frame size as well as variable brightness level using Spartan-3E Xilinx FPGA board. Specifically, we used Xilinix Spartan XC3S500E-4FG320 target platform for this implementation. The hardware performance was measured on Nexys-2 development board from Digilent Inc. The white LED light switching was done using a MOSFET in series with the LED light and gate terminal of MOSFET was driven directly from FPGA board IOs. The optical receiver used is based on Toshiba's optical fiber module TORX-173, which has built in binary detector and provides digital output. The binary detector behavior can be modeled as maximum likelihood ratio detector. The data transmission was performed at 500kHz clock due to the switching frequency limitation of the LED light source. However, it is worth mentioning that encoder/decoder performance was satisfactorily evaluated at 50 MHz clock using wired link from transmitter to receiver, demonstrating high reliability of hardware implementation.

Using NRZ (non-return to zero) ON-OFF signaling, VR-MPPM encoded signals are generated using the Xilinx's FPGA board. Encoded signals from FPGA board are fed to IRF-520 MOSFET, which is responsible to drive the LEDs. The data transmission rate is 5×10^5 bps. Output from the optical receiver (TORX173) is in digital format and is fed directly to the FPGA board. To determine the symbol error rate a total of 10^6 different symbols are transmitted, at the given brightness level, while the erroneous symbols are enumerated at the receiver. The ratio of the number of erroneous symbols to the total number of symbols transmitted provides the symbol error probability. For a given value of n, the above procedure is repeated for different brightness levels and the results obtained are shown in Fig. 5. From the result in Fig. 5 we observe that the symbol error probability is low when B_I is close to either 0 or 1 and increases as B_I is changed to take values closer to the mid point ($B_I = 0.5$). The larger symbol error probability, for B_I approximately 0.5, points toward the bandwidth limitation as well as saturation of the receiver module. Using the expression in (5), we define symbol error probability to acount for receiver saturation as

$$p_e = 1 - (1 - \bar{p}_1)^{n-r}(1 - \bar{p}_2)^r. \tag{11}$$

In (11) $\bar{p}_1$ and $\bar{p}_2$ are defined as $B_I p_1$ and $(1 - B_I)p_2$, which account for receiver saturation. The variables p_1 and p_2 are constant bit error probabilities. Defining $\bar{p}_2$ as $(1 - B_I)p_2$ models the phenomenon that an increase in the value of B_I results in reduction in the probability of decoding a pulsed slot as non-pulsed slot because of receiver saturation. Opposite is the case for the non-pulsed slots. Using this fact, symbol error probability defined in (11) is also plotted in Fig. 5 alongside experimental results. The theoretical curves match well with experimental results for different values of n.

When the data transmission rate is increased, we anticipate an increase in the bit error rate. One of the sources of bit error rate increase is attributed to the LED bandwidth limitation. Another reason for an increase in bit error rate is due to the receiver saturation as well as its limited dynamic response.

V. Conclusions

We propose variable-rate multi-pulse-position-modulation (VR-MPPM), for LED based visible light communication system, to achieve joint brightness and data transmission rate control. Unlike conventional solutions, employing two

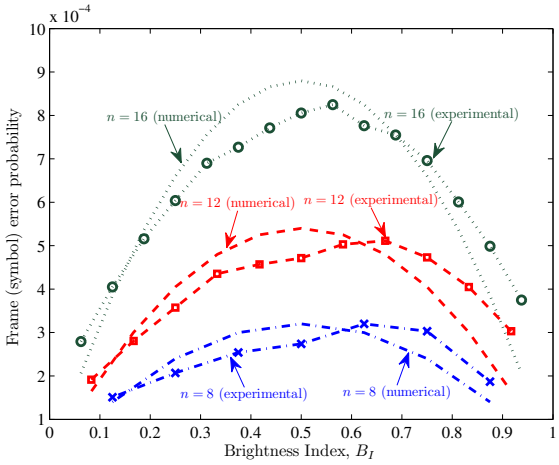

Fig. 5. Experimental evaluation of symbol error rate as a function of B_I for different values of frame size, n.

different modulation schemes one for brightness control and the other for data transmission, the proposed solution achieves the dual objective by using single modulation scheme. The brightness control resolution depends on the frame word size used by VR-MPPM and the achievable code-rate for data transmission depends on the number of pulsed slots per symbol. Lower and upper bounds for code-rate performance are derived. Iterative algorithms for encoder and decoder implementation are developed. We have also developed a hardware testbed and experimental results are obtained to quantify the effect of brightness-index on the symbol error rate performance.

The current decoder implementation, using least significant bit first approach, requires complete frame reception before the decoding can start and results in a delay equivalent to one frame transmission time. This delay can be avoided by using MSB first implementation of the decoder, however it requires the value of parameter r known to the receiver a priori. This requirement limits the possibility of changing the brightness level on the go.

REFERENCES

[1] E. Schubert and J. Kim, "Solid-state light sources getting smart," *Science*, vol. 308, no. 5726, pp. 1274–1278, 2005.
[2] N. Narendran and Y. Gu, "Life of LED-based white light sources," *J. Display Technol.*, vol. 1, no. 1, pp. 167–171, 2005.
[3] M. Doshi and R. Zane, "Control of solid-state lamps using a multi-phase pulse width modulation technique," *IEEE Trans. Power Electron.*, vol. 25, no. 7, pp. 1894–1904, 2010.
[4] J. Garcia, M. Dalla-Costa, J. Cardesin, J. Alonso, and M. Rico-Secades, "Dimming of high-brightness LEDs by means of luminous flux thermal estimation," *IEEE Trans. Power Electron.*, vol. 24, no. 3-4, pp. 1107–1114, 2009.
[5] Y. Fang, S.-H. Wong, and L. Hok-Sun Ling, "A power converter with pulse-level-modulation control for driving high brightness LEDs," in *Proc. 2009 IEEE Applied Power Elect. Conf. Expo.*, pp. 577–581.
[6] Y. Kozawa and H. Habuchi, "Enhancement of optical wireless multi-pulse PPM," in *Proc. 2008 IEEE Global Commun. Conf.*, pp. 1–5.
[7] F. Xu, M. Khalighi, and S. Bourennane, "Coded PPM and multipulse PPM and iterative detection for free-space optical links," *IEEE/OSA J. Optical Commun. Netw.*, vol. 1, no. 5, pp. 404–415, 2009.
[8] H. Sugiyama and K. Nosu, "MPPM: a method for improving the band-utilization efficiency in optical PPM." *J. Lightw. Technol.*, vol. 7, no. 3, pp. 465–472, 1989.
[9] J. Garrido-Balsells, A. Garcia-Zambrana, and A. Puerta-Notario, "Variable weight MPPM technique for rate-adaptive optical wireless communications," *Electron. Lett.*, vol. 42, no. 1, pp. 43–44, 2006.
[10] S. Rajagopal, R. D. Roberts, and S.-K. Lim, "IEEE 802.15. 7 visible light communication: modulation schemes and dimming support," *IEEE Commun. Mag.*, vol. 50, no. 3, pp. 72–82, 2012.
[11] K. Lee and H. Park, "Modulations for visible light communications with dimming control," *IEEE Photon. Technol. Lett.*, vol. 23, no. 16, pp. 1136–1138, 2011.
[12] H. Park and J. R. Barry, "Modulation analysis for wireless infrared communications," in *Proc. 1995 IEEE Int. Conf. Commun.*, vol. 2, pp. 1182–1186.
[13] H. Sugiyama, S. Haruyama, and M. Nakagawa, "Brightness control methods for illumination and visible-light communication systems," in *Proc. 2007 IARIA Int. Conf. Wireless Mobile Commun.*, pp. 78–78.
[14] Y. Zeng, R. Green, S. Sun, and M. Leeson, "Tunable pulse amplitude and position modulation technique for reliable optical wireless communication channels," *J. Commun.*, vol. 2, no. 2, pp. 22–28, 2007.
[15] M. Tahir and A. B. Siddique, "Optimal brightness-rate control using VR-MPPM and its spectral analysis for VLC system," *IEEE Commun. Lett.*, vol. 16, no. 7, pp. 1125–1128, 2012.
[16] E. F. Beckenbach and G. Pólya, *Applied Combinatorial Mathematics*. Wiley, 1964.
[17] R. Velidi and C. Georghiades, "On symbol synchronization of MPPM sequences," *IEEE Trans. Commun.*, vol. 46, no. 5, pp. 587–589, 1998.
[18] H. Park, "Performance bound on multiple-pulse position modulation," *Optical Rev.*, vol. 10, no. 3, pp. 131–132, 2003.
[19] M. Dyble, N. Narendran, A. Bierman, and T. Klein, "Impact of dimming white LEDs: chromaticity shifts due to different dimming methods," in *Proc. 2005 SPIE Optics Photonics Conf.*, p. 59411H.
[20] S. Levada, M. Meneghini, E. Zanoni, S. Buso, G. Spiazzi, and G. Meneghesso, "High brightness in GAN LEDs degradation at high injection current bias," in *Proc. 2006 IEEE Int. Reliability Physics Symp.*, pp. 615–616.
[21] M. Simon and V. Vilnrotter, "Performance analysis and tradeoffs for dual-pulse PPM on optical communication channels with direct detection," *IEEE Trans. Commun.*, vol. 52, no. 11, pp. 1969–1979, 2004.
[22] S. Boyd and L. Vandenberghe, *Convex Optimization*. Cambridge University Press, 2004.

Abu Bakar Siddique received his B.Sc. and M.Sc. degrees in electrical engineering from the University of Engineering and Technology, Lahore, Pakistan, in 2006 and 2012, respectively. From January 2006 to Feburary 2013, he worked for Pakistan Telecommunication Company Limited (PTCL) as Operations Engineer in CDMA based wireless local loop (WLL) networks, serving in the BSS, NSS, NOC, and IN departments. Currently, he is a faculty member at the University of Management and Technology Lahore. His current research interests include coding theory and wireless personal area networks.

Muhammad Tahir is an Associate Professor at the Department of Electrical Engineering of the University of Engineering and Technology Lahore, Pakistan. Previously, he was a postdoctoral research fellow at the Institute of Microelectronics and Wireless Systems, the National University of Ireland.

He received his Ph.D. in electrical and computer engineering from the University of Illinois at Chicago (2004–2008). Dr. Tahir is the co-recipient of the Outstanding Student Paper Award in the 21st IEEE International Conference on Advanced Information Networking and Applications (2007). His research interests include delay constrained wireless networks, distributed network resource optimization, and real-time wireless multimedia networks. He has more than 30 international publications to his credit. He is a reviewer for numerous IEEE journals and conferences.